Chinese Chemical Letters 32 (2021) 1177–1180

Contents lists available at ScienceDirect

Chinese Chemical Letters

journal homepage: www.elsevier.com/locate/cclet

Communication

A facile and controllable one-pot synthesis approach to amino-functionalized hollow silica nanoparticles with accessible ordered mesoporous shells

Shaoxin Deng[a,b], Cheng-Xing Cui[b,c], Lu Liu[b], Lingyao Duan[b], Jichao Wang[b], Yuping Zhang[b,*], Lingbo Qu[a,c,**]

[a] Postdoctoral Station of Food Science and Engineering, College of Food Science and Engineering, Henan University of Technology, Zhengzhou 450001, China
[b] Postdoctoral Research Base, School of Chemistry and Chemical Engineering, Henan Institute of Science and Technology, Xinxiang 453003, China
[c] College of Chemistry, and Institute of Green Catalysis, Zhengzhou University, Zhengzhou 450001, China

ARTICLE INFO

Article history:
Received 13 July 2020
Received in revised form 13 August 2020
Accepted 3 September 2020
Available online 5 September 2020

Keywords:
Hollow silica
One-pot approach
Solid-to-hollow transformation
Ordered mesoporous shell
Amino functionalization

ABSTRACT

The development of a practical synthetic method to functionalize hollow mesoporous silica with organic groups is of current interest for selective adsorption and energy storage applications. Herein, a facile and controllable one-pot approach for the synthesis of monodisperse amino-functionalized hollow mesoporous silica nanoparticles is presented. A novel solid-to-hollow structural transformation procedure of the silica nanoparticles is presented. The structural transformation is easily designed, as observed through transmission electron microscopy, by tailoring the HCl and *N*-lauroylsarcosine sodium molar ratio and the water content in the sol-gel. Ordered and radially oriented *in situ* amino-functionalized mesochannels were successfully introduced into the shells of the hollow silica nanoparticles. A formation mechanism for the hollow mesoporous silica materials is discussed.

Porous materials of various desired components, such as porous metal oxides, porous carbon, porous silica, and even porous composite materials, are widely used in numerous applications as sensing and catalysis, as a result of their unique porous structures [1–5]. From a structural point of view, nanomaterials can be divided into dense nanoparticles [6], core/shell structure [7], hollow structure [8], and so on. Among the numerous structural porous material types, hollow structural mesoporous silica nanoparticles (HMSNs) that present permeable ordered mesoporous thin shells, high surface areas, low densities and good biocompatibilities, have received a wealth of interdependent research [9,10]. However, the intrinsic inert inorganic -Si-O-Si- framework in hollow silica limits its use in further applications. Hence, designing well dispersed organic functional groups into the inert framework of the hollow mesoporous silica is a major research goal.

Three major approaches have been developed, hitherto, to synthesize hollow mesoporous silica: i) the hard template method, ii) the selective etching method, and iii) the soft template method. The hard template method is based on the deposition of a silica precursor onto pre-prepared sacrificial particles, and thereafter, removal of the central sacrificial particle resulting in the hollow structure [11]. Adopting hard template synthetic method has one major disadvantage: challenges remain to synthesize hollow samples having accessible ordered mesopores on the shell with functionalized mesochannels. The selective etching method is an alternative synthetic strategy, where the interior walls of pre-prepared mesoporous silica materials [12], or core-shell and hybrid silica materials [13,14], are selectively etched to form hollow structures. By adopting the selective etching strategy, the preparation of organic groups functionalized hollow mesoporous silica generally requires bis-silylated organosilanes as the silica precursor [15]. The synthetic approach required tedious modification and needed selective etching of the particle interior, which is cumbersome, time-consuming, and uneconomical. The soft template method prepares hollow silica materials generally through the self-assembly of silicate species and surfactants at the emulsion droplet/water interface [16], vesicles/water interface [17], gas bubbles/water interface [18] and micellar aggregates/

* Corresponding author.
** Corresponding author at: Postdoctoral Station of Food Science and Engineering, College of Food Science and Engineering, Henan University of Technology, Zhengzhou 450001, China.
E-mail addresses: zhangyuping@hist.edu.cn (Y. Zhang), qulingbo@zzu.edu.cn (L. Qu).

https://doi.org/10.1016/j.cclet.2020.09.002
1001-8417/

water interface [19]. The soft template method has been demonstrated to be a powerful method because of its unrivalled advantage in fabricating hollow materials with accessible ordered mesoporous shells. Yet despite literatures exist [20], there remain significant challenges to realize simpler and more practical approaches for the preparation of functionalized hollow silica with ordered mesoporous shells.

Herein, a facile and controllable one-pot method to synthesize monodisperse amino-functionalized HMSNs is reported. A novel solid-to-hollow structural transformation procedure is established by varying the HCl and the anionic surfactant *N*-lauroylsarcosine sodium (Sar-Na) molar ratio together with the water content. In this synthetic method, the ordered and radially oriented meso-channels on the shells of the hollow silica nanoparticles were *in situ* functionalized with amino.

For brevity, the HCl and Sar-Na molar ratio, and the volume of water were labeled as *X* and *Y* (mL), respectively. Fig. 1 presents the transmission electron microscopy (TEM) images of the calcined samples prepared as a function of *X* and *Y*. In Fig. 1a, the monodisperse sample particles, prepared at *X* = 0.3 and *Y* = 30, are observed to possess a dense solid spherical morphology. The solid particle diameters are in the range of 200∼400 nm, measured directly from the TEM images. The solid silica materials have radially oriented mesochannels (Fig. 1b), which was further confirmed by small angle X-ray diffraction (XRD). As shown in Fig. 2, the sample prepared at *X* = 0.3 and *Y* = 30 exhibits three well-resolved XRD diffraction peaks. These diffraction peaks can be indexed to the (100), (110) and (200) characteristic diffractions of the 2D hexagonal mesostructure. However, interestingly, the

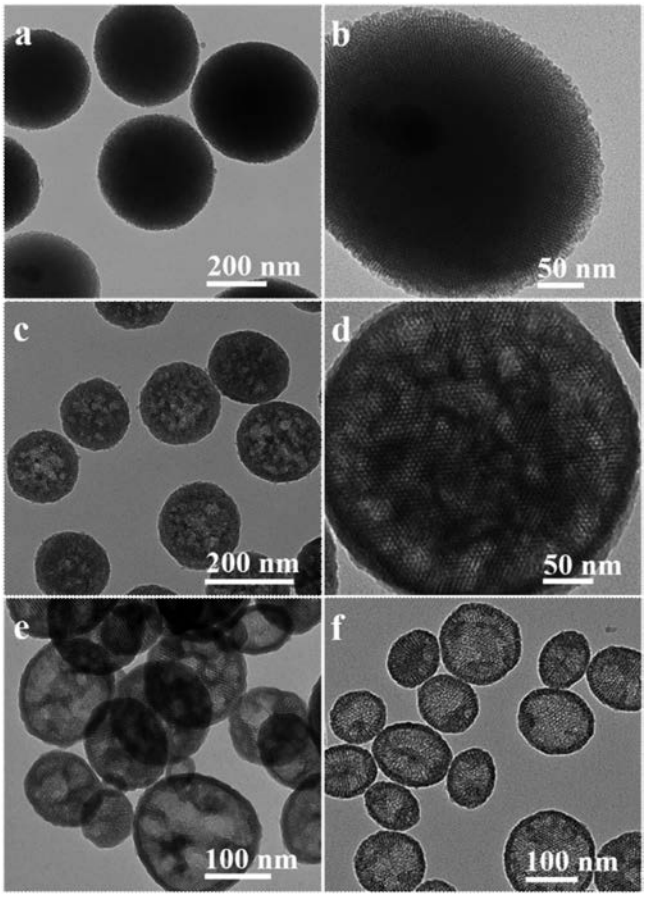

Fig. 1. TEM images of the calcined samples prepared as a function of HCl and Sar-Na molar ratio (*X*) and water content (*Y*). (a, b) *X* = 0.3 and *Y* = 30; (c, d) *X* = 0.2 and *Y* = 30; (e) *X* = 0.2 and *Y* = 80; (f) *X* = 0.2 and *Y* = 100.

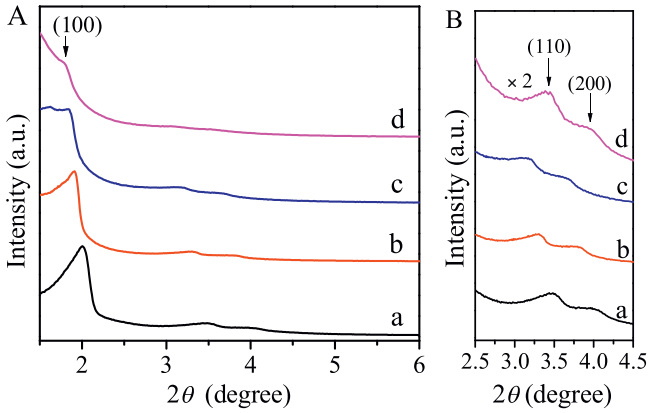

Fig. 2. Small angle X-ray diffraction patterns of the calcined samples synthesized as a function of HCl and Sar-Na molar ratio (*X*) and water content (*Y*). (a) *X* = 0.3 and *Y* = 30; (b) *X* = 0.2 and *Y* = 30; (c) *X* = 0.2 and *Y* = 80; (d) *X* = 0.2 and *Y* = 100. (B) is the enlarged view of (A) ranging from 2.5°-4.5°.

sample was not observed to exhibit a dense solid particle when *X* was reduced to 0.2 with all other experimental conditions unchanged. As shown in Fig. 1c, the sample interior exhibits numerous closely arranged areas of lesser density of varying size. The particle size distribution basically conforms to the normal distribution (Fig. S1 in Supporting information), and the particle diameters mainly lie in the range of 150∼350 nm. Furthermore, the particles exhibit a highly ordered 2D hexagonal mesoporous channels arrangement (Fig. 1d), which also was confirmed by the XRD patterns, as shown in Fig. 2.

As the water content increased, the internal structure of the product significantly changed. As shown in Figs. 1c and d, when *Y* is 30, the particle interiors possess numerous closely arranged areas of lesser density. However, when *Y* was increased to 80, the areas of lesser density, located within the particle interior, are observed to be interconnected and separated only by a thin mesoporous wall (Fig. 1e). Furthermore, thin spherical shells are clearly observed at the particle boundaries leading to almost hollow interiors. The particle diameters and shell thicknesses are in the range of 100∼200 nm and 5∼15 nm, respectively. Importantly, the particles prepared at *X* = 0.2 and *Y* = 80 exhibit highly ordered mesochannels, which is confirmed by small angle X-ray diffraction, as shown in Fig. 2. As *Y* is further increased to 100, well-defined HMSNs, with large inner cavities and ordered mesoporous shells, were formed. The hollow structure of this sample is confirmed by TEM imaging, which demonstrates a noticeable contrast in electron density between the core and the shell. The particle diameters and shell thicknesses are 100∼150 nm and ∼10 nm, respectively. As shown in Fig. 2, the sample prepared at *X* = 0.2 and *Y* = 100 also exhibit three resolved characteristic diffraction peaks, indicating that the shell of the hollow silica has ordered mesochannel arrangement.

SEM images (Fig. S2 in Supporting information) show that the obtained samples generally consisted of spherical nanoparticles. And a decrease in particle size is observed when the water content is increased, which is consistent with the results of TEM micrographs.

The N_2 adsorption-desorption isotherms of the calcined samples synthesized as a function of *X* and *Y* are shown in Fig. 3A. The adsorption isotherms of all the samples show typical IV isotherms. The inflection point related to the rapid uptake of the adsorbate at a relative partial pressure between 0.3–0.5 P/P_0, reveals the materials having a narrow pore size distribution. This result is consistent with the pore size distributions (Fig. 3B). Each of the pore size distributions has a narrow peak and pore size

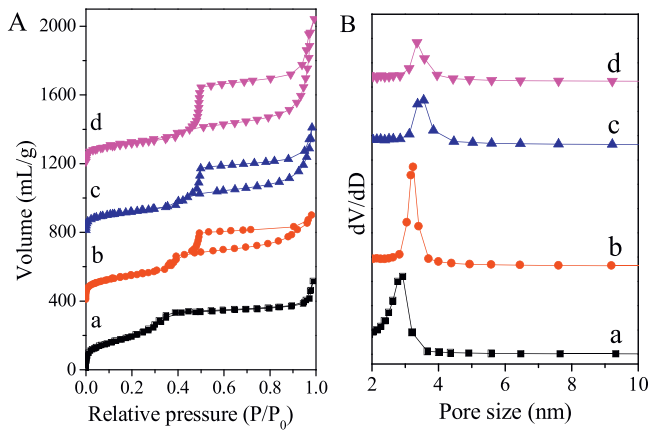

Fig. 3. (A) N_2 adsorption-desorption isotherms and (B) pore size distributions of the calcined samples prepared as a function of HCl and Sar-Na molar ratio (*X*) and water content (*Y*). (a) *X* = 0.3 and *Y* = 30; (b) *X* = 0.2 and *Y* = 30; (c) *X* = 0.2 and *Y* = 80; (d) *X* = 0.2 and *Y* = 100.

centrated at about 3.0 nm. Additionally, the N_2 adsorption-desorption isotherm of the sample synthesized at *X* = 0.2 and *Y* is 30, 80 or 100 has a hysteresis loop, while the sample prepared at *X* = 0.3 and *Y* = 30 did not exhibit a hysteresis loop. Furthermore, the hysteresis loop becomes more prominent as *Y* is increased. This type of hysteresis loop is H2 type [21], which also been observed for other hollow structures with mesoporous shells [18,22]. It is probably due to the delay of nitrogen evaporation from the hollow voids blocked by the surrounding mesopores during the N_2 desorption process [18]. These results further indicate that the synthetic silica particles underwent a structural transformation from solid to hollow, which is in agreement with the TEM observations. Furthermore, the obtained mesoporous silicas possess high surface areas and large pore volumes. The specific surface area of the calcined hollow silica was 423.8 m^2/g, which was calculated by Brunauer-Emmett-Teller (BET) method.

Based on the above experimental results, a possible formation mechanism of HMSNs is proposed. Fig. 4 presents a schematic illustration for the formation process of the hollow mesoporous silica. Herein, hollow mesoporous silica was fabricated by using the anionic Sar-Na surfactant as the template, 3-aminopropyltrimethoxysilane

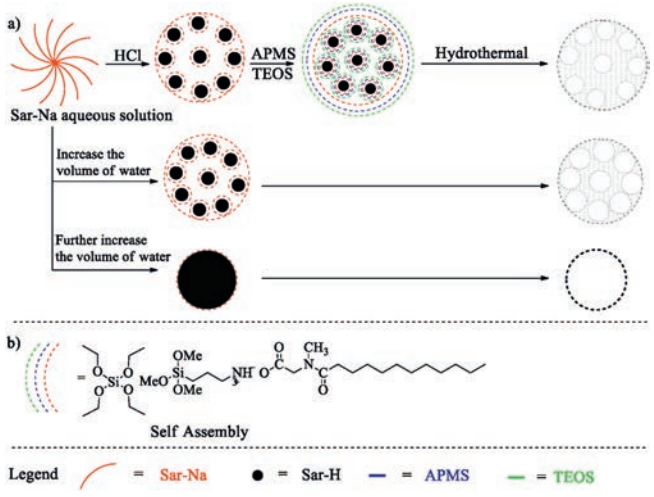

Fig. 4. Schematic illustration for the formation process of the hollow mesoporous silica nanoparticles.

(APMS) as the co-structural directing agent (CSDA), through a $S^-N^+I^-$ pathway, where S is the surfactant, N is the CSDA, and I relates to the inorganic precursors [23]. Co-structural directing agent was used to assist the electrostatic interaction between the silica precursor and the negatively charged surfactant. A portion of Sar-Na is converted to *N*-lauroylsarcosine (Sar-H) when an appropriate amount of HCl was added to the aqueous solution comprising Sar-Na. Sar-H is an oily substance, which forms small oil droplets in aqueous solutions. Each oil droplet is suggested to be stabilized by Sar-Na at the oil/water interface. APMS is concentrated at the oil–water interface when added, and thereafter, is protonated because of acid-base neutralization. Subsequently, the oil droplets are expected to act as a "nucleus" for the interfacial self-assembly. During the self-assembly process, the positively-charged amine sites of the protonated APMS interact electrostatically with the templating anionic surfactant micelles, and simultaneously the alkoxysilane sites of the protonated APMS co-condense with the silica precursor [23]. Therefore, due to the existence of the oil droplet "nucleus", the resulting self-assembly products are not dense solid particles, but the particles interior exhibits numerous holes. Furthermore, the silica particle diameters decrease as a function of increased water content, as shown in the previous TEM (Fig. 1) and SEM (Fig. S2) micrographs. However, the oil droplet size remains essentially unchanged. Therefore, the distance between the oil droplets decrease when residing within the small silica particle interior. Finally, well-defined hollow structures were obtained. At elevated temperatures during hydrothermal treatment, the initially formed silica/surfactant hybrid mesophase underwent a structural transformation to yield an outer shell possessing ordered and radially oriented mesochannels [24].

As mentioned above, the hollow mesoporous silica was fabricated through a $S^-N^+I^-$ pathway. During the self-assembly process, the positively-charged amine sites of APMS interact electrostatically with the templating anionic surfactant micelles, and simultaneously the alkoxysilane sites of APMS co-condense with the silica precursor. After removing the anionic surfactant by extraction, the *in situ* functionalized material is rendered porous and the amino groups derived from APMS reside within the mesoporous shell. Hence, the hollow silica material presents a homogeneous distribution of the amino groups located at the mesoporous surface. Fourier transform infrared (FT-IR) spectra of the as-synthesized and the extracted samples are presented in Fig. S3 (Supporting information). The peaks at 2854 and 2925 cm^{-1} are assigned to the C-H vibrations of the surfactant. The intensities of the two peaks are observed to decrease after acid extraction, indicating the efficient removal of the surfactant. Compared with the as-synthesized sample, the sample after acid extraction exhibits a large characteristic peak at 3500–3300 cm^{-1}, corresponding to the N-H infrared characteristic stretching vibration peak of the primary amine. The results clearly indicate the successful amino functionalization of the hollow mesoporous silica.

In summary, a facile and controllable one-pot approach is presented for the preparation of amino-functionalized hollow mesoporous silica nanoparticles. The findings suggest that the HCl and Sar-Na molar ratio and the water content are two crucial factors to tailor the final structure of the products. Our synthesis approach realizes simpler and more practical preparation of functionalized hollow silica with accessible ordered mesoporous shells, avoiding tedious modification and manipulation for multifunctional applications. Furthermore, the hollow particles prepared herein will be of interest for the fabrication of various multifunctional silica-based hollow nanocomposites because of the radially oriented amino-functionalized mesochannels.

Declaration of competing interest

The authors report no declarations of interest.

Acknowledgments

We gratefully acknowledge the support of National Natural Science Foundation of China (No. 51802082), Training Plan for University's Young Backbone Teachers of Henan Province (No. 2019GGJS170), Science and Technology Research Project of Henan Provincial Science and Technology Department (No. 142102210047), The New Century Excellent Talent Support Program for Colleges and Universities in Henan Province (No. 2006HANCET-01) and "Climbing" Project of Henan Institute of Science and Technology (No. 2018CG04).

Appendix A. Supplementary data

Supplementary material related to this article can be found, in the online version, at doi:https://doi.org/10.1016/j.cclet.2020.09.002.

References

[1] J. Qin, B.S. Li, D.P. Yan, Cryst. 7 (2017) 89–99.
[2] T. Zhao, P.P. Qiu, Y.C. Fan, et al., Adv. Sci. 6 (2019) 1902008.
[3] T.F. Gao, A. Kumar, Z.C. Shang, et al., Chin. Chem. Lett. 30 (2019) 2274–2278.
[4] T. Zhao, Y. Ren, G.Y. Jia, et al., Chin. Chem. Lett. 30 (2019) 2032–2038.
[5] P.P. Qiu, T. Zhao, J. Khim, et al., J. Materiomics 6 (2020) 45–53.
[6] R.Z. Liang, R. Tian, Z.H. Liu, D.P. Yan, M. Wei, Chem. Asian J. 9 (2014) 1161–1167.
[7] W.H. He, Y. Yang, L.R. Wang, et al., ChemSusChem 8 (2015) 1568–1576.
[8] M. Arif, G. Yasin, L. Luo, et al., Appl. Catal. B 265 (2020) 118559.
[9] J. Hu, M. Chen, X.S. Fang, L.M. Wu, Chem. Soc. Rev. 40 (2011) 5472–5491.
[10] L. Yu, X.Y. Yu, X.W. Lou, Adv. Mater. 30 (2018) 1800939.
[11] E.M. Schneider, S. Taniguchi, Y. Kobayashi, et al., ACS Sustainable Chem. Eng. 5 (2017) 4941–4947.
[12] L.L. Fu, S.F. Zhao, Y. Chen, Z.G. Liu, Chem. Commun. 52 (2016) 5577–5580.
[13] A. Yildirim, M. Bayindir, J. Mater. Chem. A 3 (2015) 3839–3846.
[14] X.W. Liu, G.G. Qian, Z. Jiao, M.H. Wu, H.J. Zhang, Chem. Eur. J. 23 (2017) 8066–8072.
[15] W.P. Fan, N. Lu, Z.Y. Shen, et al., Nat. Commun. 10 (2019), doi:http://dx.doi.org/10.1038/s41467-019-09158-1.
[16] N. Ma, Y.Q. Deng, W.T. Liu, et al., Chem. Commun. 52 (2016) 3544–3547.
[17] J.J. Wang, W. Xiao, J.Q. Wang, J.M. Lu, J.H. Yang, Mater. Lett. 142 (2015) 269–272.
[18] J.G. Wang, F. Li, H.J. Zhou, et al., Chem. Mater. 21 (2009) 612–620.
[19] J. Hu, X. Wang, L.Q. Liu, L.M. Wu, J. Mater. Chem. A 2 (2014) 19771–19777.
[20] Y.Y. Sun, M. Chen, L.M. Wu, J. Mater. Chem. A 6 (2018) 12323–12333.
[21] K.S.W. Sing, D.H. Everett, R.A.W. Haul, et al., Pure Appl. Chem. 57 (1985) 603–619.
[22] B. Tan, H.J. Lehmler, S.M. Vyas, B.L. Knuston, S.E. Rankin, Adv. Mater. 17 (2005) 2368–2371.
[23] S. Che, A.E. Garcia-Bennett, T. Yokoi, et al., Nat. Mater. 2 (2003) 801–805.
[24] H. Wang, J.G. Wang, H.J. Zhou, et al., Chem. Commun. 47 (2011) 7680–7682.